Tracking DENV-3 Dynamics: A Focused Study on Its Emergence as the Second Most Circulating Serotype During Dengue Epidemics

Sayma Nasrin Shompa

International Islamic University Chittagong, Computer Science and Engineering, Chittagong, Bangladesh

Abstract

There are four different types of dengue virus, or Denv, which are Denv-4 from Denv-1, and it is still a major public health issue worldwide. Recently, Denv-3 has appeared more often in outbreaks, usually coming as the second most often identified type. This paper sees the factors of genetic, ecological and epidemiology that affects how Denv-3 behaves. By analyzing recent outbreaks in Asia and Latin America through molecular and spatial methods, we can see how the Denv-3 capacity is increasing due to epidemics. Conclusions highlight how important genomic tracking and effective vector management approaches are.

Many studies have seen various serotypes, but they often use samples that do not lend themselves to understand how the virus spreads over time in an urban area. In this research, we check how the different lineages of Denv-3 were broadcast during 2006 in Sau Jose Do Rio Preto, Brazil. We collected blood samples from patients who showed symptoms like dengue and demonstrated M-N-PCR, to detect and identify the virus using primers based on NS5 genes. The resulting pieces were purified and indexed, and we lived positive dengue cases. To classify sequined samples, we aligned them with 52 reference sequences. This dataset was then used to reconstruct reconstruction phylogenetic on the basis of maximum probability method. We estimated the best demographic model, growth rate, evolutionary change rate and time for the most recent general ancestor (TMRCA). We also estimated the basic fertility rate during the outbreak. Of the 174 blood samples, we received sequences from 82 patients and successfully lived 46 of those sequences. The alignment obtained a dataset of 399 nucleotides with 134 taxes. Phylogenetic analysis showed that all samples were of Denv-3 and belonging to strains from Martinec Islands between 2000 and 2001. In particular, 60 Denv-3 samples of Sao Jose Do Rio Preto formed a monophyletic group (dynasty 1), which belonged to near 22 other isolated (clan 2).

We believe that these dynasties emerged on different occasions before 2006. By converting the approximate exponential growth rate in the basic fertility rate, we calculated the R0 values of 1.53 for the lineage 1 and 1.53 for the lineage 2. Under the exponential model, the TMRCA for the dynasty 1 was about one year old, while the dynasty 2 was dated to 3.4 years ago from the previous sample. Genetic data often unlike the ability to understand spatial-temporal dynamics, but it can provide valuable insights on how DENV is transmitted. By combining geographical and temporarily structured phylogenetic data, we got a clear picture of how at least two dengue spread viral strains in densely populated urban areas.

Denv for dengue virus, or short, comes in four types, Denv-1 to Denv-4, and it is a major health issue worldwide. Recently, Denv-3 has emerged as the second most prevalent type in various epidemic areas, so it is important for us to closely monitor its transmission. The study takes a close look at Denv-3's genetic and time-related patterns during the outbreak in 2006 in 2006, Sao Jose Do Rio Preto, Brazil. Using the M-N-PCR targeting NS5 genes, we identified and indexed viral samples from 82 dengue positive patients, in which 46 cases were ground coded for spatial analysis. Phylogenetic reconstruction revealed two different monophyletic genealogies of Denv-3, both tracing back to strains from Martinec (2000–2001), indicating several introduction events before 2006. Importantly, for the estimated reproductive number (R_0) of lineage-specific analyzes, for the genealogy 1 and 2, respectively, 2, 2, respectively. These findings highlight the evolutionary diversity and transmission capacity of the co-circulating Denv-3 genealogy within a single urban outbreak. By integrating genomic, demographic and spatial data, our study displays the important value of future dengue epidemic more effectively and file a significant value of filing in management.

Keywords

Dengue virus, DENV-3, Serotype Emergence, Phylodynamic, Public Health, Epidemic Surveillance

1. Introduction

DF typically comes with headaches, a fluctuating fever, skin rashes, pain behind the eyes, low white blood cell counts, reduced platelet counts, and swollen lymph nodes. On the flip side, DHF is characterized by high fever, bleeding symptoms, and signs of circulatory failure [1]. While many molecular phylogenetic studies have looked into various dengue serotypes [2,3,4], there's still a lack of detailed research focusing on specific outbreaks in urban settings with fine spatial and temporal granularity [5,6].

Patients with these symptoms can end with hypovolemic shock, which can cause DSS, which can be fatal. Outside Africa, the primary vector for dengue transmission is Aedes Aegypti mosquito, which thrives in all tropical and subtropical regions [7,8].

Nearly three billion people are at risk of DENV infection. In 2007, Brazil accounted for about 94.5% of reported dengue cases in Central and South America, and around 60% of cases globally [9].

Roughly three billion people are at risk of dengue infection. In 2007, Brazil accounted for about 94.5% of reported dengue cases in Central and South America and 60% worldwide. Up until the 39th epidemiological week of that year, there were 481,316 cases of DF reported in Brazil, from a population of around 186 million, alongside 1,076 instances of DHF [9]. São Paulo State, home to 21% of Brazil's population, contributed to 17% of these cases (82,684) [9].

Many molecular phytology studies have been performed to understand the various dynamics of dengue serotypes [10,6]. However, there is still a difference in understanding specific outbreaks in urban settings with detailed spatial and cosmic analysis [5,11,12]

In this study, we delve into the spread patterns of distinct lineages of the DENV-3 virus during the 2006 outbreak in São José do Rio Preto, São Paulo, Brazil, and look into the outbreak's dynamics and microevolution [13,14,15].

In this work, we discuss that in 2006, Sau Jose Do Rio Preto, Sao Paulo, Brazil analyzed separate lineage of the Denv-3 virus spread during the outbreak of 2006, analyzing the dynamics and microevolutions in that period. The dengue virus (Denv) has four different serotypes (Denv-1 to Denv-4), each displaying the dynamics of unique evolutionary and epidemiology. Of these, Denv-3 has recently shown a disturbed revival in several urban centers, which has become the second most prevalent serotype during recent outbreaks.

What makes this study unique is that it digs into the phylodynamic and microevolution of DENV-3 during a particular outbreak, the 2006 epidemic in São José do Rio Preto, São Paulo, Brazil. Unlike previous research that tends to generalize findings across regions or serotypes [16,17,18], we offer a detailed analysis of how DENV-3 emerged as the second most common serotype during this specific epidemic, including important spatial and temporal factors that many previous studies have missed [19,20].

A lot of research has been done on the genetic evolution of dengue [2,7,10], but there’s still a big gap out there; most studies don't really dive into the fine details of space and time, especially when it comes to those fast-moving outbreaks in urban areas [6,11,15]. This paper aims to fill that gap [21].

In our study, we take a closer look at the DENV-3 outbreak in 2006 in São José do Rio Preto, São Paulo, Brazil an urban hotspot that felt the impact of this epidemic. Rather than looking at broader regional trends, we’re using detailed phylodynamic analysis to follow how different DENV-3 lineages came about and spread within this particular city. By focusing on such fine details, we’re not just reconstructing how the outbreak unfolded; we’re also revealing how specific lineages adapt and spread in crowded environments.

2. Materials and Methods

2.1 Study Site

The urban area is divided into the 432-census tract, which includes around 300 houses, defined by the Institute Barilaro de Geographic E Statistical - IBGE (Brazilian Institute of Geography and Statistics), which is more efficient to create data collections during census. SJRP faced an outbreak of a dengue from Aedes Aegypti in 1985, but only until 1989 was reported to be imported cases. Sao Jose Do Rio Preto (SJRP) is located in the north -west of the Brazilian state of Sao Paulo. It is about 434.10 km of size, of which 96.81 km are urban. The population was estimated to be 424,114 in 2007. With an average annual temperature of about 25 ° C, the city enjoys a tropical climate. It also receives 1,410 mm of rainfall, most of which fall during summer. SJRP has a diverse economy that incorporates industry, services, commerce and pre -run business, and its development indicators are comparable to essentially developed nations. Since 1990, when the first human-to-human transmission of Denv-1 was documented, the yearly dengue cases have been reported with the exception of 1992. Along with Denv-2 [5].

2.2 Geo-Coding

We used ArcGIS 9.0 to geo-code local dengue cases. For each patient, we assumed their location based on the latitude and longitude of their zip code, which we got from the patient address records provided by the city of São José do Rio Preto.

2.3 Sample Collection

sample collection We collected blood samples from patients who had acute fever, whether they showed symptoms of bleeding or not. Sudden infections, nausea, vomiting, diarrhea, as well as signs of dengue fever (DF) and dengue hemorrhagic fever (DHF), all were included for flavors tests in local health units and hospitals after obtaining informed consent to all. The study was approved from the Ethical Review Board at Facula de Medicine D Sao Jose Do Rio Preto, and blood collection was done with written consent.

2.4 CDNA Synthesis and Sequencing

We began by centrifuging blood samples and following their instructions, removed the viral RNA from the serum using Qi AMP viral RNA mini kit from Queen. For the first round of RT-PCR, we used flexitarian generic primers targeting non-structural protein 5 (NS5). The region is very preserved in the dengue virus, allowing us to detect most circulating dengue strains in Brazil with only one PCR step. In the second PCR, we applied multiplexes or traditional, either multiplexes or traditionally to identify the virus, with species-specific primers. For primers, we used FG1 which bids as the NS5 genes and about 958 BP. In addition, we had a specific internal primer for Denv-3 has to be produced. After purifying the pieces from the PCR mixture, we sequence them using the Big Dye V3.1 terminator kit from the applied biosystems. This was further done on the ABI377 automatic sequencer with FG1 primer and reverse Denv-3 primer. Finally, we aligned the results using Accelrys gene 2.0 software. [20,22]

2.5 Phylogenetic Reconstruction

To analyze the sequenced samples, we aligned 52 reference sequences, which included representatives from all four serotypes, using the Se-Al version 2.0a11 program (and we can provide the data if you ask). This dataset was then used to reconstruct the phylogenetic tree based on maximum likelihood criteria, employing a genetic algorithm method via GARLI version 0.95. This method helps estimate the best tree topology, branch lengths, and optimal values for the General Time Reversible (GTR) model of nucleotide evolution, which incorporates Gamma-distributed variable rates and invariant sites (so we refer to it as GTR+Γ+I). We ran GARLI independently 100 times to ensure robustness, and the tree that showed the highest likelihood was selected for further optimization using PAUP v.4.0b10. Since both GARLI and PAUP can calculate likelihood scores under the same model, this step was crucial. Finally, we assessed support for the tree topology using 100 bootstrap replicates with GARLI [23,24].

2.6 Phylodynamic of Dengue 3

For the data we analyzed, we saw three demographic models: (i) continuous population size, (ii) exponential growth, and (iii) logistic growth. We have estimated the growth rate (R = Neag) - which is an effective number of transmission phenomena multiplied by the time of the pathogen's generation - as well as the rate of evolutionary change (μ) measured in site replacement per year, and time for the common ancestor (TMRCA) recently. For this we used the biracial estimate with a Markov Chen Monte Carlo (MCMC) method available in Beast V1.6. The sequences were dated to the dates of their sample, and we run the Micmac until the effective sample size (ESS) for each parameter was stabilized above 100. We provided confidence interval for each parameter using a 95% highest probability density (HPD). The analysis consisted of a relaxed molecular clock (unrelated lagoonal) in constant, exponential and logistic demographic models. Since the priests were different, we compared the demographic model by calculating the log 10 of the Bayas factor. This was done using the hormonic medium without the sum of each coalescent and the possibility of each holstering for all models, using tracer v1.6. [25].

2.7 Analyzing Spatial-Temporal Spread Patterns

To begin, we wanted to see if our samples were either locally or temporarily structured, so we created a distance matrass to compare them. These matrixes help us understand how close each sample is for others based on their collection dates, locations and genetic information. We used PAUP to get the correct genetic distance from an estimated maximum probable tree with Garli after GTR+γ+I model. For geographical distance, we calculated the straight-line measurements between samples using geographical information systems. When the samples were collected, the temporal distance was simply the time interval. We tested the disabled hypothesis - that there is no link between genetic, geographical and temporary distances using partial mental tests. Statistical distribution was designed by calculating a partial correlation coefficient for each sequence by raising rows (and corresponding columns) in phytoclimatic distance matrix 1,000 times. A type of I was determined by checking the ratio of sorted correlation coefficients (which means dismissing a true disproportionate hypothesis) which were equal to or more than the coefficient seen. We considered the possibilities below $\alpha = 0.05$ statistically important [26].

Next, we used a straight algorithm to find out how dengue can spread to SJRP. This algorithm examines all samples (except one) in cosmic order and assumes that the first collected samples with high genetic similarity are ancestors. We have not found any significant geographical barriers in the studied field that hinders the movement of the vector or host, so we did not add any obstacles to our calculation. Instead, we set a range of 0.00739 replacement per site per year, which we thought that per site per site per year could come per site per year from the virus copying more than 100 days at the rate of 10–4 replacement per year. If any sample was not closer to this limit for any of its earlier counterparts, we concluded that it came from a separate virus introduction in that area [26].

2.8 Calculating R0 for the 2006 SJRP Dengue Epidemics

Since each viral sequence came from a different patient, we can view the nodes in the virus gene tree as transmission events in the human population. This allows us to estimate the basic reproduction number of a pathogen (R0) during an epidemic using the formula R0 = 1 + D * (ln2 / (t * d)) [27]. Here, D represents the average time someone is infectious (which is about 7 days for virus shedding in humans) [28], and t * d refers to the doubling time of the epidemic. We found that the growth rate (r) derived from viral phylodynamic equals ln2 / (t * d) [25], enabling us to estimate R0 as 1 + Dr. However, the typical population growth models (like exponential or logistic) available in BEAST don't accurately

reflect the fluctuating dynamics we saw during this outbreak, which could impact the growth rate estimates from these models. This was reinforced by the changing nature of the Bayesian skyline (BSL) plot for dengue, which indicated a rapid increase at the start of the epidemic followed by a decline in cases towards the end. To tackle this, we also explored a different method for estimating R0, focusing solely on the growth phase of the epidemic. This involved deriving the force of infection during the rising phase of the BSL. We fitted the normalized median of the Bayesian estimates from the analyzed sequences, y(t), to a continuous logistic curve based on our model [27,29].

$$y(t) = \frac{1}{1+\exp(3-8.5\times10^{-6}t^2)} \quad (1)$$

You can use equation (1) to estimate the infection force based on the data[30,29].

$$\lambda(t) = \frac{dy(t)}{dt}\frac{1}{(1-y(t))} \quad (2)$$

Where,

$$\frac{dy(t)}{dt} = \frac{(1.7\times10^{-4})\exp(3-8.5\times10^{-6}t^2)t}{(1+\exp(3-8.5\times10^{-6}t^2))^2} \quad (3)$$

The Basic Reproduction Number, known as R0, was derived from the average rate of infection. This was based on equation (2), which relates to the number of new cases occurring over a specific time period among those who are susceptible, as outlined in a previous study [28].

$$R_0 = 1 + \frac{\lambda^2 + \lambda(\mu+\gamma)}{\mu\gamma} \quad (4)$$

Here, μ refers to the mosquito mortality rate, while γ represents the recovery rate of viraemia in humans. Essentially, the mosquito mortality rate indicates how quickly mosquitoes tend to die over time; it's the opposite of how long, on average, a specific mosquito population lives. This rate can vary depending on where you are, and even in the same region, it might shift due to things like temperature, rainfall, and other climate-related factors. For our study, we decided to go with a mosquito mortality rate of about 2.23×10-2 per day, which is what was estimated for the SJRP before [28].

3. Results and Discussion

3.1 Dengue Characterization and Sequencing

We ended up with 399 bp-long sequences of a part of the NS5 gene, which we got from the viral genomic RNA directly taken from the blood of 82 patients. These samples came from 198 collected between January 12 and June 5, 2006, during a time when cases were peaking in São José do Rio Preto—specifically, in April 2006, when there were more than 1000 cases for every 100,000 residents (GenBank accession numbers EU715692 to EU715773). Out of the 82 patients, we could geo-locate 46 based on their home addresses, but we couldn’t do the same for the other 36 because we didn’t have their full addresses.

3.2 Dengue Typing and Origin

We compared 82 sequences against 52 references, which helped us create a 399-nucleotide-long dataset without any gaps, covering 134 taxa. Initial phylogenetic analysis, which included all four serotypes, indicated that every sample belonged to serotype 3 (though we won't show that data here). All our samples clustered within DENV-3, showing a close relationship with strains that were found in Martinique during 2000 and 2001, as well as with the DENV-3 strain Den3_BR74886 that circulated in Brazil in 2002 (see Figure 1). Additionally, it seems that, based on the reference samples we analyzed, the South American lineages are more closely related to lineages from Southeast Asia. Another notable discovery was that 60 DENV-3 samples from SJRP formed a tight-knit group (lineage 1, shown in blue), with a 90% posterior probability. This group was closely related to 22 other isolates that didn't fit into a clear monophyletic cluster (lineage 2 and 3, shown in orange), which positioned themselves more basally on the tree and mixed with other South American references from Martinique and Brazil.

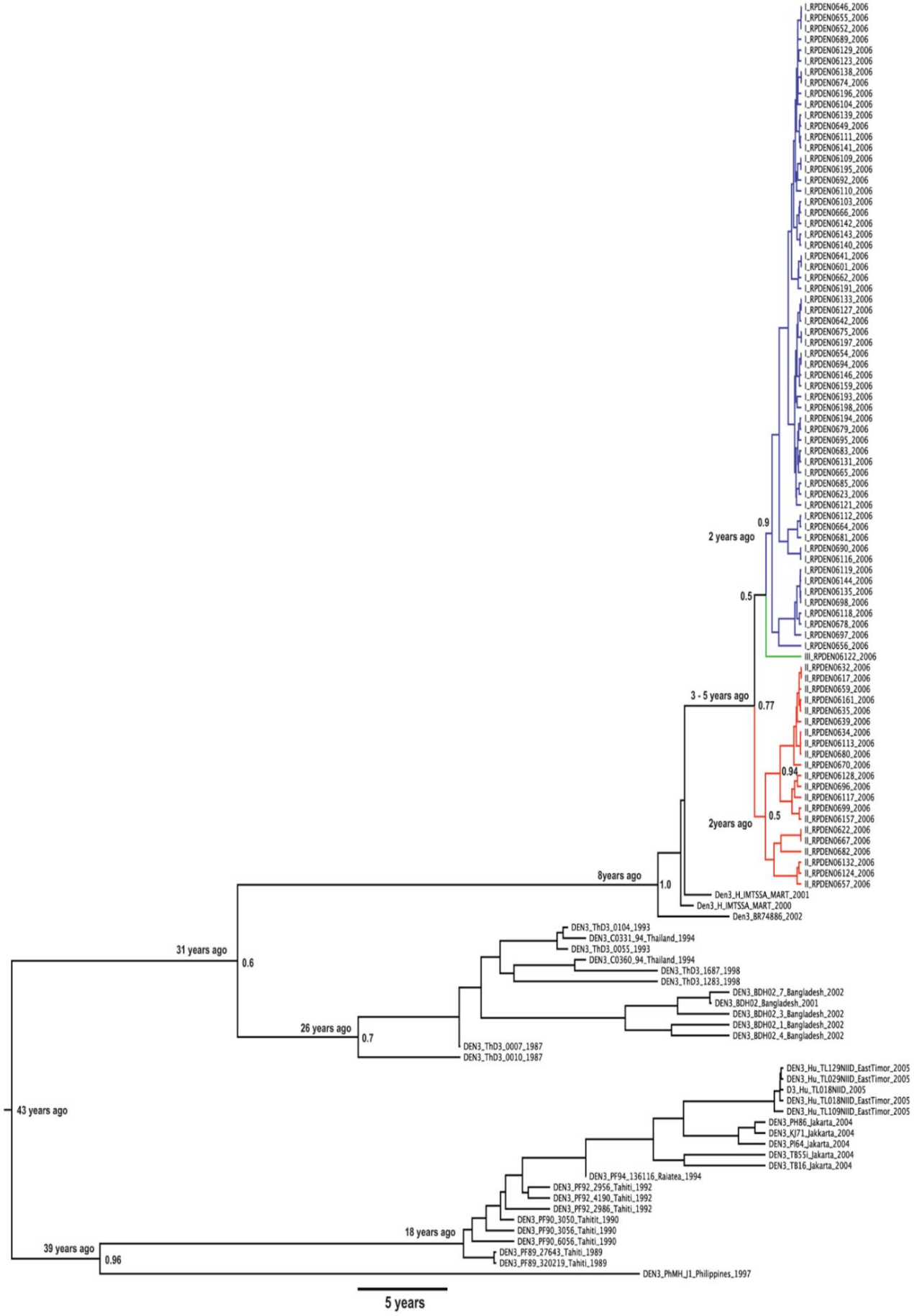

Figure 1. The maximum clad reliability of 131 global dengue virus serotype 3 exposes Tree 3 isolates lineage relations and ancestral origin

Figure 1 shows the maximum clade credibility (MCC) tree for 131 Dengue 3 isolates. This MCC tree, based on samples from various locations around the world, suggests that the 60 lineage 1 samples are likely derived from lineage 2 viruses, which have a 77% posterior probability support. Notably, the closely related BR47886 strain, collected in 2002 in Brazil, along with the H IMTSSA strain from 2000 in Martinique, are positioned at the base of the SJRP lineages, supported by a 100% posterior probability. https://doi.org/10.1371/journal.pntd.0000448.g001

3.3 DENV-3 Dynamics in SJRP

We analyzed demographic data using a bison skyline with the animal, which allowed us to create a maximum clad reliability (MCC) tree that shows dated tips and internal nodes. The tree suggested that both genealogies deviate 1 to 3 years before the last sample taken in SJRP (see Figure 1). Since we did not inspect the outbreak of any ongoing DENV-3 during this time limit in SJRP, we felt that the possibility of these genealogies emerged before the 2006 season, possibly being introduced in the area at different times. Therefore, we considered these major genealogies as a separate viral population in our subsequent demographic analyzes. In particular, most of the lineages shown in orange in Figure 1 shared a general ancestor with a backward potential of 77%, allowing us to create a group as a lineage 2 for these analyzes. Both sample groups showed significant population growth about six months before the previous sample - this very well aligns with reports showing an increase above 100,000 per 10 cases in December 2005 (Figure 2). In addition, we rejected the continuous population size model for both the Denv-3 dynasty (for the dynasty 1, 10 Beys Factor> 250, for the lineage 2, 10 Beys Factor> 146). While in Figure 2, the tendency of the Biercean skyline plot appears logistic to the summit of the outbreak, the logistics model did not perform better than the inverted growth model for either the dynasty 1 (log 10 bays factor = 23.9) or dynasty 2 (Log 10 Bays Factor = -436). In fact, even though the logistics model obtained a high bays factor (146.251) compared to the exponential (150.686), and adding more logistic parameters did not improve the details of the data meaningfully. It is important to note that the highest post -density (HPD) indicated the growth rate (R) for both lineage (R).

The effective sample size (ESS) dynasty was 107.75 for 150,400,000 states for 1 and 325,600,000 for the descent 2 for 1239.444 for states for 150,400,000 states. When we converted these projected experiencedly growth rates into basic reproductive numbers, we found 1 (for a 95% HPD range) to Linz 1 (for a 95% HPD range) and HPD range above 1 to 1.3). Even though we rejected the logistics model, the original fertility rate obtained from its growth rate (not shown here) was with R0 = 3.765 dynasty 1 (95% HPD range from 1 to 9.554) and the dynasty 2 (95% HPD range from 1 to 8.896) for R0 = 3.093). This suggests that the growth rate was about 50% higher during the exponential growth in the dynasty 1, but only 17% higher when using the logistic model. Under the exponential model, two years ago the most recent common ancestor (MRCA) for the dynasty 1 (MRCA), and the dynasty 2 also dated two years from previous samples (with 95% HPD between 6 months and 5 years) for the dynasty 1, two years ago from the last sample (with 95% HPD between 6 months and 3 years). Overall, it seems that both genealogies show similar development patterns, but descent 1 strains grow rapidly (and there is a high R0). A defect of the earlier approach is that the monotonic models used in the animal (logistic and experienced) would not have captured the correct ups and downs of the epidemic, as they fail to reflect the decline in new infections after the outbreak summit. To address this, we discovered alternative methods [28,30,29,31]. The viral genealogy for the logistics fit y (T) for the Biercean skyline plot is estimated in Figure 3A. We estimated the original reproductive number, R. from the average force of the infection (Figure 3B), calculated from the equation (2), which according to the susceptible individuals give us 0.17 new cases per time, based on the pre - proposed method [28]. From equation (4), we received R0 = 2.45. Conclusions indicate a concrete agreement between the values obtained directly from the estimated growth rate with animals, which are calculated using the force of infection, and the estimates of epidemiology of 3.36 were earlier prescribed before double time of cases were determined earlier.

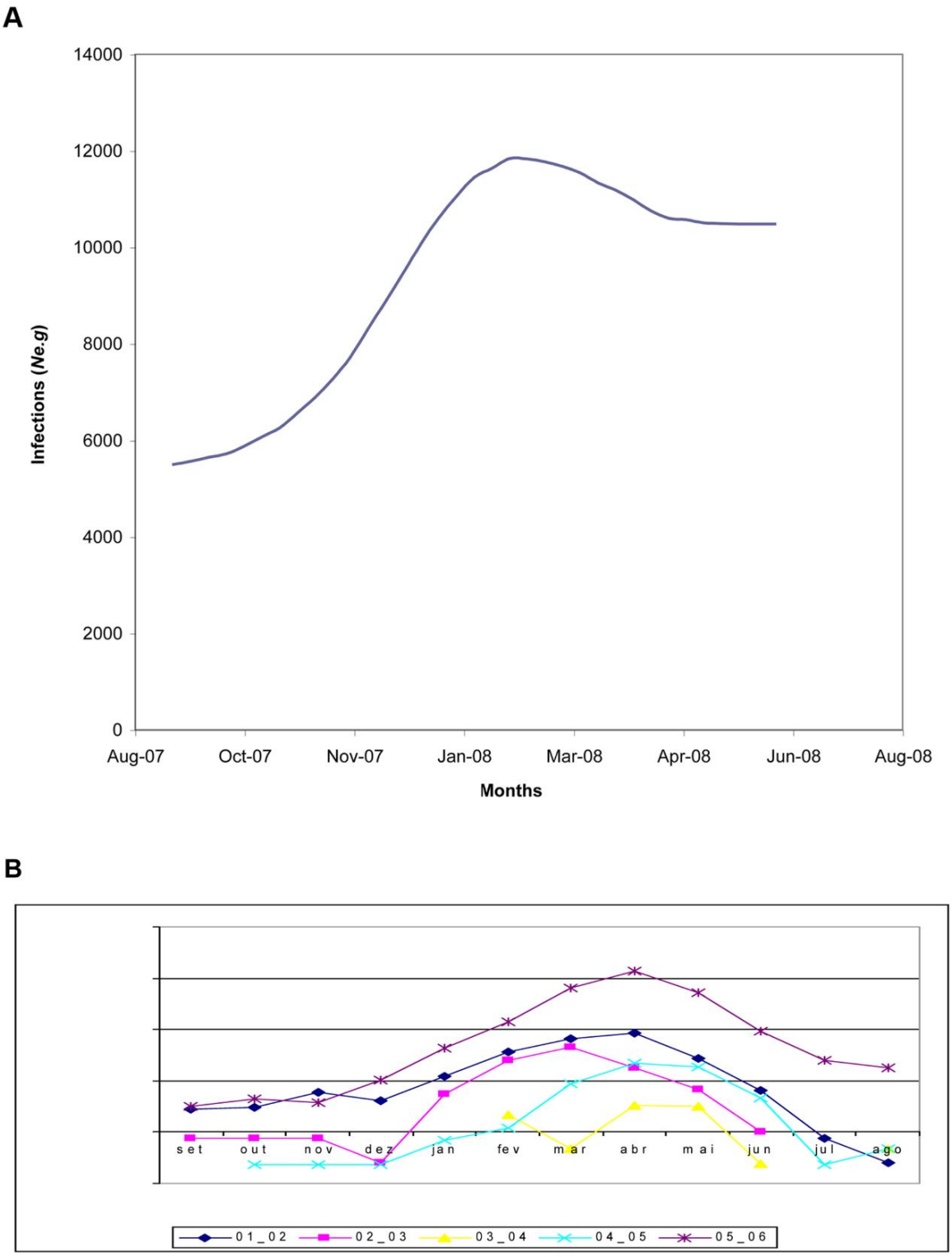

Figure 2. Dengue cases reported in the Bayesian Skyline Plot and SJRP (2001-2006): Denv-3 infections and temporary mobility of epidemic peaks

Figure 2 shows the Bayesian skyline (BSL) plot alongside the number of dengue cases reported. A) The BSL plot presents a genealogy-based estimate of new infections, indicated as Neag, and illustrates the median for 82 DENV-3 isolates. Any noticeable changes in total population sizes can largely be attributed to the BSL showing the total count of new infections, along with possible scaling issues or errors in reporting. The data shows that infections rose from 180 to 120 days prior to the last sampling date, which we're calling day 0. This uptick corresponds quite well with the increase in reported cases per 100,000 people that began in December 2005. Looking at the number of dengue cases reported in SJRP from the 2001–2002 season through to the 2006 season, it's clear that the highest number of cases in 2006 happened in April, which matched up with the peak of the epidemic around February, as suggested by the Bayesian skyline plot. https://doi.org/10.1371/journal.pntd.0000448.g002

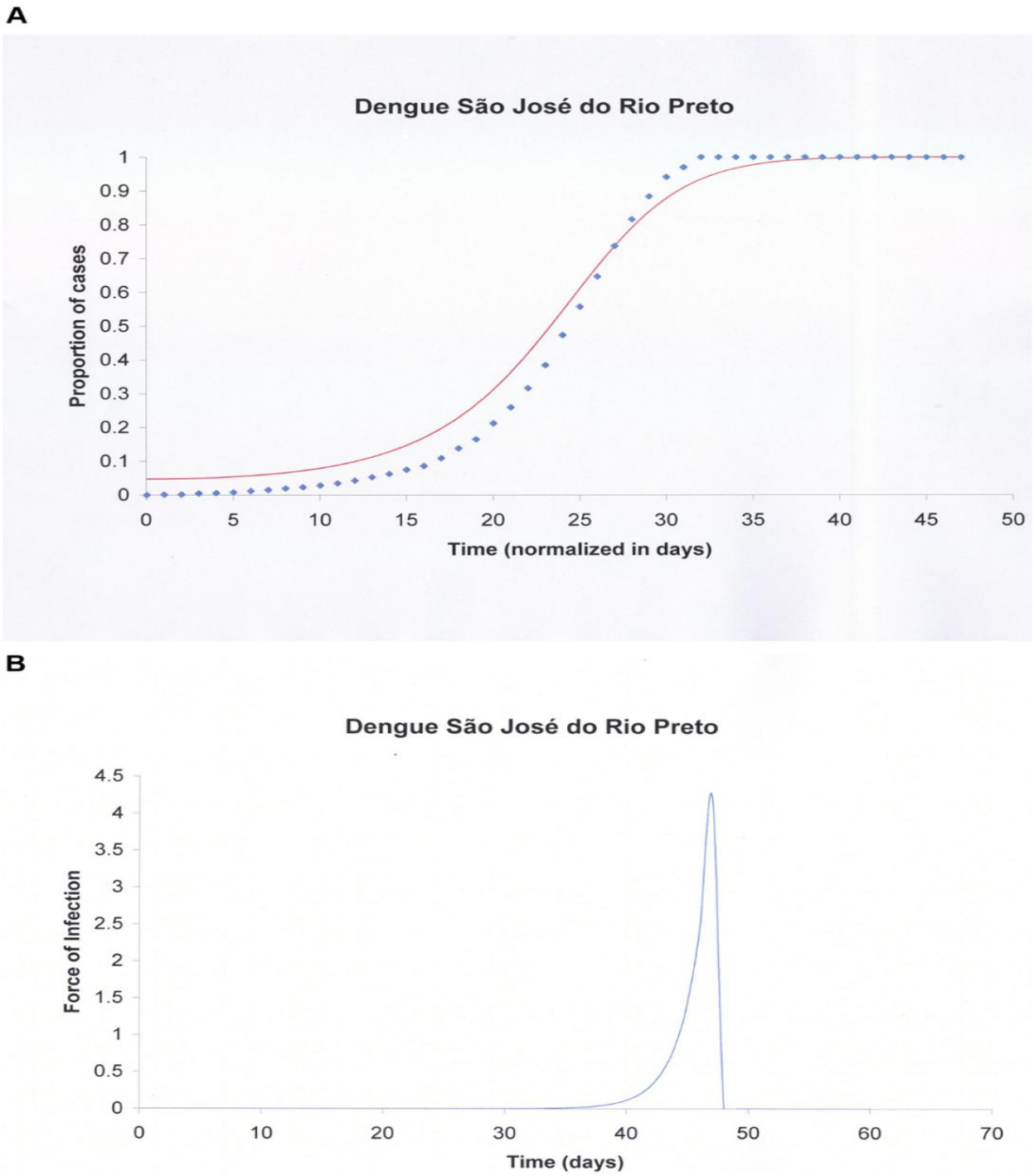

Figure 3. Logistic growth fit and inferior transmission from Dynamics by Bayesians Skyline Estimates (A) The BioScan Skyline Plot, the generalized secondary estimation from Y (T) Y (T), was fitted for a logistic development model representing the epidemic expansion phase in early 2006. Diamonds indicate sequence-rich data points; The solid curve shows logistic fit. (B) Estimated force of infection over time, derived from logistic model using equation (2)

Figure 3 shows how the Bayesian skyline plot fits into a logistic model and the force of infection.

(A)Here, you can see the normalized median from the Bayesian estimates of the sequences we analyzed, y(t), matched to a continuous logistic curve based on equation (1). The diamonds indicate the data points, while the continuous line represents the function we've fitted. This time frame covers the epidemic during the fat growing phase in January and February of 2006. B) The force of infection is derived from the model we fitted in part A) using equation (2). https://doi.org/10.1371/journal.pntd.0000448.g003

3.4 Spatial-Temporal Distribution of DENV-3 Lineages in SJRP

When we took a look at the matrix of the distance trimmed by time in Figure 4, we saw a bright patches in the same 'block -light -matrix with some genetically similar -the first matrix was aligned with the temporal gradients seen in the matrix. However, they were mixed with dark lines that indicated less genetic proximity. It seems that this mixture of genetically distant samples threw a wrench in the overall statistical association. This was likely to be due to various

genealogies roaming together in the SJRP during the outbreak. In addition, there was actually no spatial union between samples (as shown in the third matrix) when we compared others. Our visual raids were supported by statistical analyzes, which were detected between the very low -spearman correlations between the matrices (R = 0.06 with geographic and R = 0.01 with the cosmic), both were not important (<0.05 depending on the mental method with 1,000 interaction) [26].

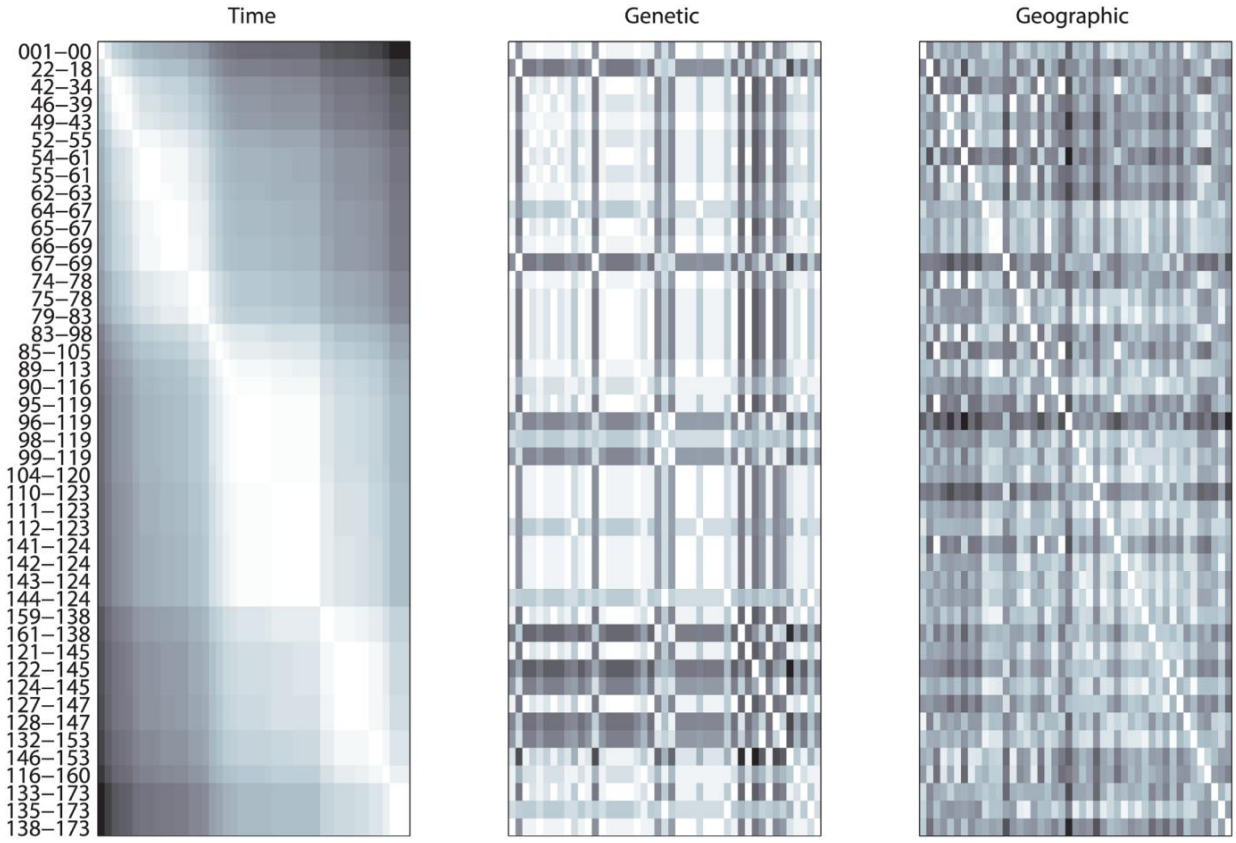

Figure 4. Symptomatic distance mates reflecting temporary, genetic and spatial relationship between 46 samples Represent heatmaps (A) Temporal, (B) genetic, and (C) spatial distance, with a color gradient from white (low values) to black (high values). The samples are temporarily ordered, which increases the visual interpretation of the distance pattern in the matrass

Figure 4 shows symmetrical matrices. These matrices illustrate: A) temporal, B) genetic, and C) spatial distances between the 46 samples. To make comparisons easier, we've replaced the numbers with a color scale, where white indicates lower values and black represents higher values. The samples are arranged temporally, which you can see in the gradual pattern in matrix A), and the colors used for the sample names help highlight the comparisons with the results.

The analysis using what's called the 'nepotistic algorithm' showed there were at least three separate introductions of strains from lineages 1 and 2 into SJRP. These lineages seem to match up pretty well with the tree in Figure 1. The spatial-temporal relationships are depicted in three dimensions in Figure 5, which helps clarify why there wasn't a clear statistical link among the correlation matrices. You can see the three main virus introductions as clusters of genetically similar strains mixed in with more distantly related ones in the genetic distance matrix shown in Figure 4. In fact, those 'darker lines' line up with the lineage names highlighted in red in Figures 4 and 5. If you look a bit closer, you'll notice that, just like we saw with the 'blue' samples from lineage 1, the genetic distances among the 'red samples' were also pretty low. The branching pattern of the spatial-temporal tree in Figure 5, created with the 'nepotistic algorithm,' helps explain why there wasn’t any correlation between the geographic distance matrix and the other distances. It turns out the virus is spreading from three distinct starting points, rather than following a single outward pattern. https://doi.org/10.1371/journal.pntd.0000448.g004

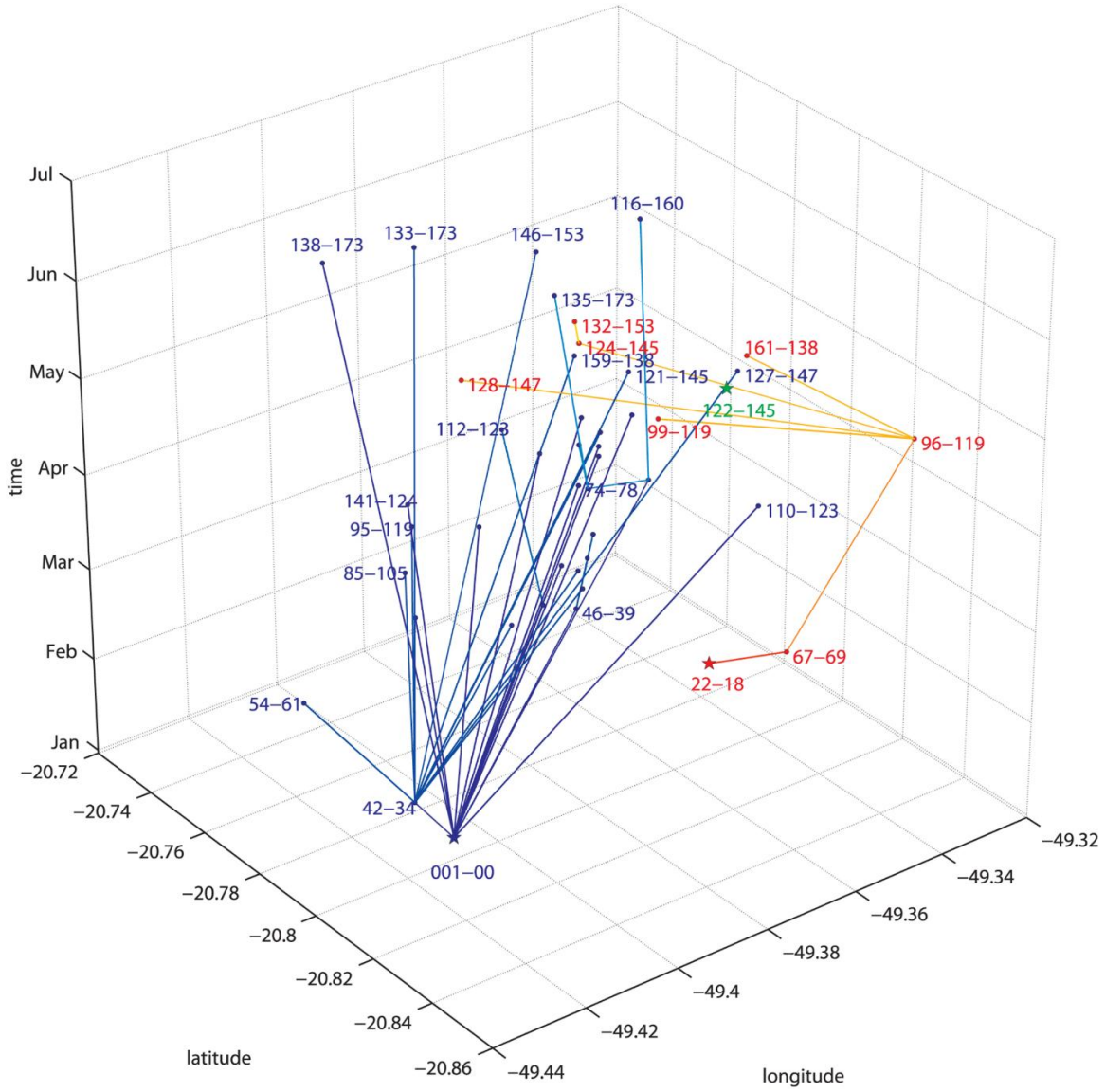

Figure 5. the estimated paths of dengue spread based on the "Nepotistic algorithm." https://doi.org/10.1371/journal.pntd.0000448.g005

In this three-dimensional graphic, the base represents the geographical coordinates of where the samples were collected, while the vertical axis indicates the months during which sampling took place. Each unique lineage starts with a "star" marking the oldest sample for that lineage, and the lines connecting to other samples (with names placed as closely to the points as possible) vary in width, reflecting how genetically related the samples are. There are three lineages shown: (i) the green lineage, which is the most recent and has just one sample, labeled 122-145; (ii) the red or "South-eastern" lineage, which starts with sample 22-18 and then shifts to yellow for more recent ancestry; and (iii) the blue, or "North-western" lineage 1, beginning with 01-00 and lightening up, similar to the previous one.

The 'North-western' part (lineage 1) highlighted in blue in the spatial-temporal trees in Figures 5 and 6 included the earliest samples collected on January 12th. It was also the most common, with 36 samples, and it lasted the longest, as it also covered the five most recent samples: ‘138-173’, ‘146-153’, ‘116-160’, ‘133-173’, ‘135-173’, and another ‘138-173’, which were collected between June 14th and July 4th. The lineage 1 samples were connected by an average distance of 3.25 kilometers, with a range from just 15 meters to 7.23 kilometers. The rate of spread averaged around 67.3 meters per day, although it varied quite a bit from just 18 centimeters per day for two samples (‘95-119’ and ‘42-34’) that were only 15 meters apart, to a maximum of 428.8 meters per day. Interestingly, some lineage 1 samples appear to be key sources for several others, with sample names and the number of links generated as follows: ‘01-00’: 16; ‘42-34’: 12; ‘64-67’: 2; ‘90-116’: 2; and ‘98-119’: 2. On the other hand, the 'South-eastern' samples, grouped into at least lineage 2 and shown in red in the spatial-temporal tree (Figures 5 and 7), had fewer components, only 8 samples. Their activity was recorded from January 30th (‘22-18’) to June 14th (‘132-153’). The average distance between their connections was 4.7 kilometers, ranging from 0.2 to 8.7 kilometers, with an average spread speed of 152 meters per day (minimum of 28 meters/day and maximum of 311 meters/day). The '122-145' sample (Figures 5, 6, and 7) may represent another introduction of dengue into SJRP.

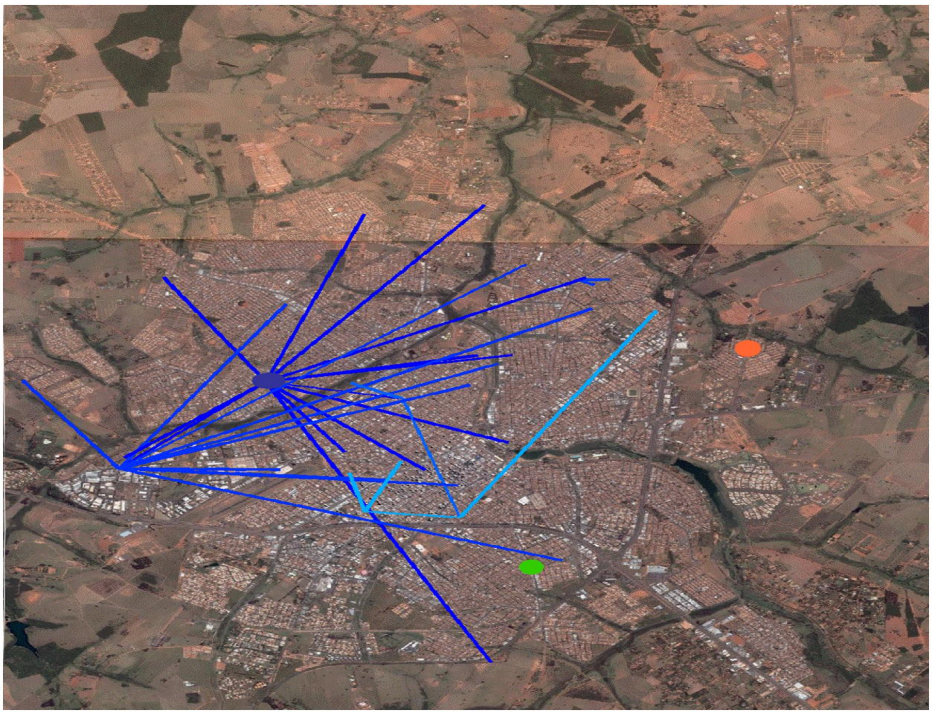

Figure 6. Estimated spatial route of 'North Western' dengue strain This figure shows the approximate geographical trajectory of the 'North-Western' dengue strain, which originates from its reinforced ancestral node (blue dot) and moves towards various reported case places. Light colored lines indicate more recent transmission events. A green dot marks the sample with a third distinct viral introduction. (Background imagery: Google Earth V4.2.0181.2634, Downloaded on 16 September 2007.)

Figure 6. Path of viral spread - I. This shows the estimated path of the 'North-western' strain starting from its supposed ancestor (marked by the blue dot) and spreading to various locations where dengue cases have been reported. The lines leading to more recent nodes appear in lighter shades. Also included is a green dot representing the sample from the third viral introduction. (The background image came from Google Earth version 4.2.0181.2634, which was downloaded on September 16, 2007.) https://doi.org/10.1371/journal.pntd.0000448.g006

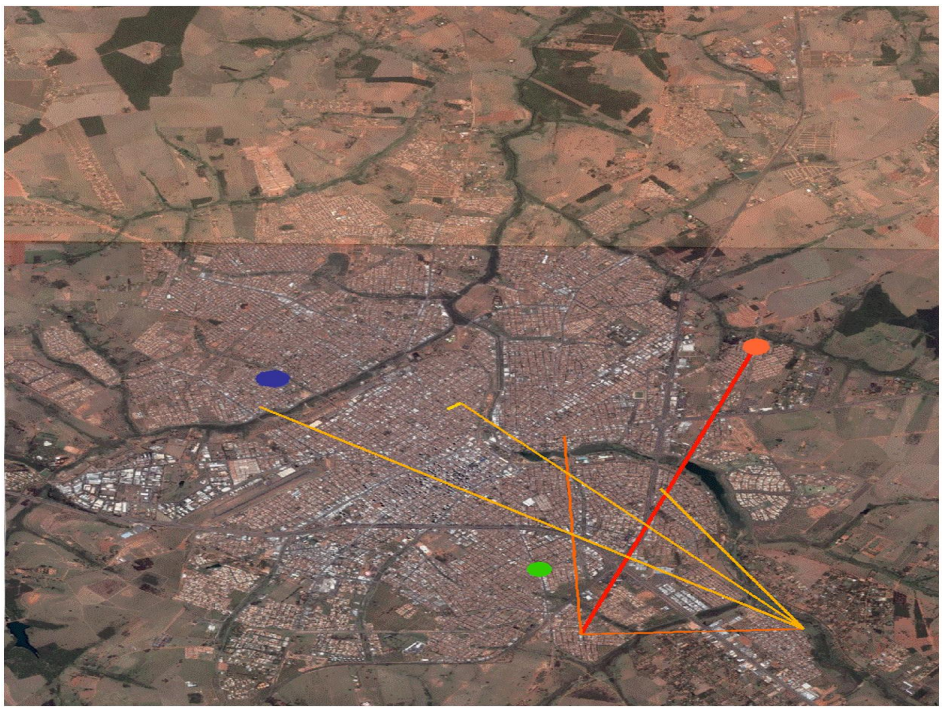

Figure 7. Path of viral spread - II. https://doi.org/10.1371/journal.pntd.0000448.g007

This shows the estimated journey of the 'South-eastern' strain, starting from its likely ancestor (marked with an orange dot) and moving out to various locations where dengue cases have been reported. The lines that lead to more recent nodes are shaded in yellow. You can also see the sample from the third viral introduction represented by a green dot. (The background image is sourced from Google Earth 4.2.0181.2634, downloaded on September 16, 2007.)

3.5 Socioeconomic Features

Figure 8 shows the confirmed cases of dengue in the local area reported by the Surveillance Service from September 2005 to February 2006. In September 2005, there were dengue cases in an irregular residential area called Santa Clara, located in the northern part, just outside the city limits, where basic sanitation is pretty much nonexistent. Over the following months, the number of cases in that neighborhood increased, and the disease began to spread into other urban areas. We did some molecular testing on the strains detected and found at least three different viral introductions: 01-00, 22-18, and 122-145. The first outbreak was in Eldorado, a neighborhood known for its low socioeconomic status. Other cases popped up in neighborhoods with varying socioeconomic conditions (see Figures 5, 6, and 9). There was a notable cluster of cases in Gonzaga de Campos, which is a working-class area located near the main industrial zone, involving cases 42, 85, 95, and 141. After that, more cases tied to case 42 spread to other areas with different socioeconomic statuses (again, see Figures 5, 6, and 9). Case 22-18 led to additional infections within lineage 2, except for case 122-145, which also came from São Diocletian, another low-income area. Interestingly, a connection was found between the socioeconomic status of the census tracts and the incidence rates according to what was reported by the Surveillance System (Table 1). Even though the positive RT-PCR cases were spread evenly across different census tracts (Table 1 and Figure 9), about 44% of the low socioeconomic census tracts fell into the highest incidence quartile, while only 5.5% of the high socioeconomic tracts found themselves in the same situation.

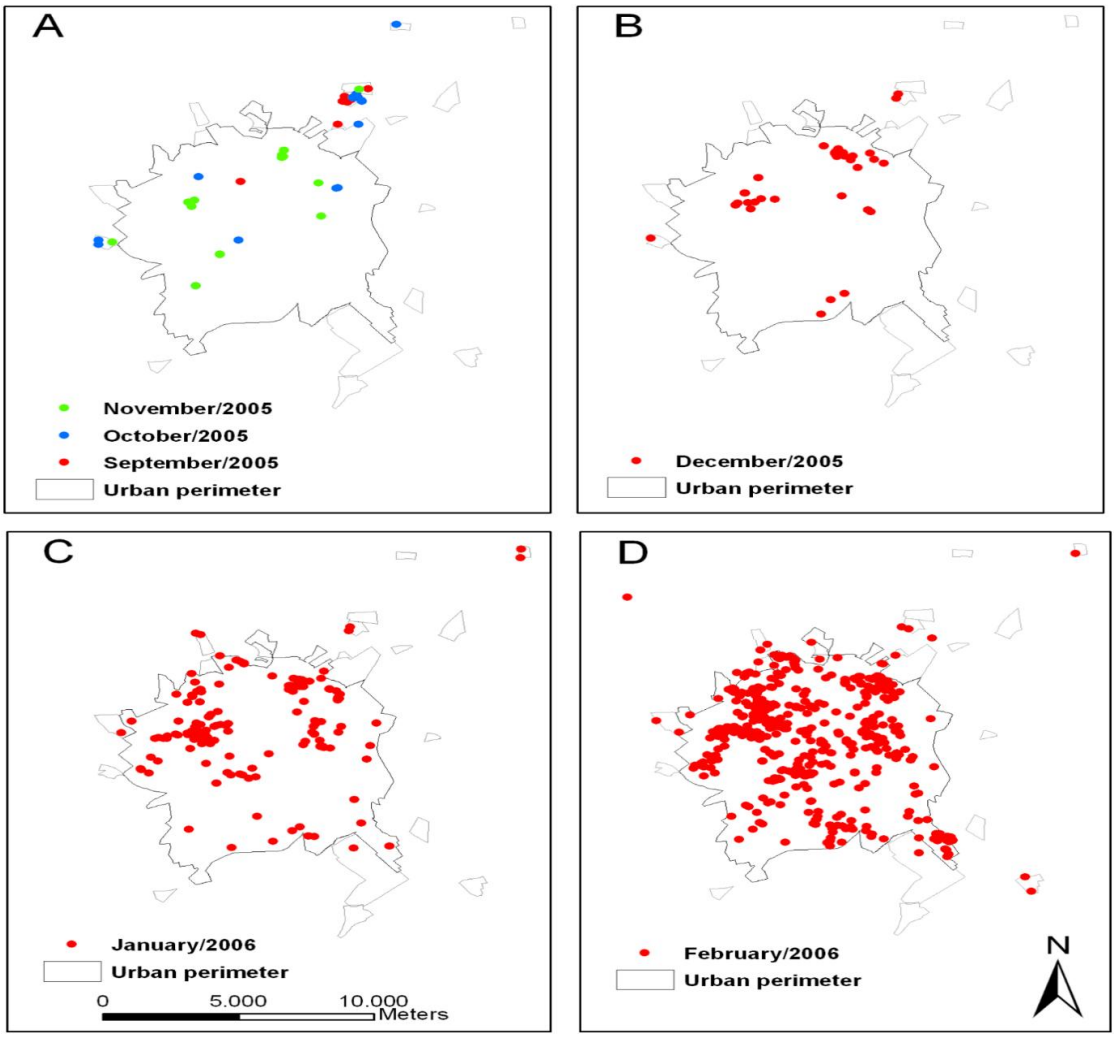

Figure 8. The spatial distribution of dengue cases confirmed in Sao Jose is Rio Preto till the month (September -February), highlights urban census tract and irregularly developed areas

Check out Figure 8: it's a map of São José do Rio Preto. It marks the urban census tracts, spots with irregular development, and confirmed dengue cases reported by the Surveillance System from September to November (A), December (B), January (C), and February (D). The areas outside the city's urban limits are kind of developed in an irregular way, looking a bit like urban zones, but they lack proper sanitation systems and typically deal with tougher socioeconomic conditions than the urban census tracts. Notably, in September 2005, there was a cluster of cases in one of these irregular areas in the North Zone (Santa Clara), which later spread to the neighboring urban areas (A). https://doi.org/10.1371/journal.pntd.0000448.g008

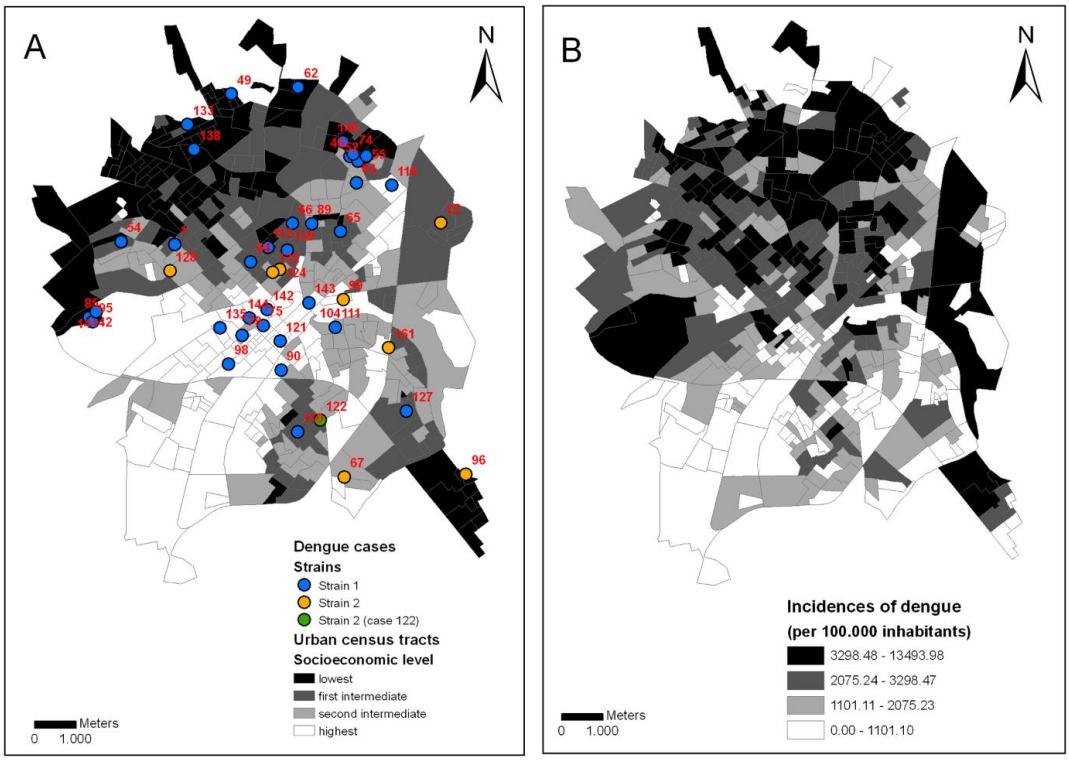

Figure 9. Social economic stratification and dengue incident in urban census tract, (B) The rate of dengue incidents was given to the monitoring system in the same urban census paths from September 2005 to August 2006

Figure 9 shows urban census tracts, which are basically continuous and uniform areas made up of about 300 buildings on average (IBGE 2002). It classifies these areas based on socioeconomic levels (quartiles) and the dengue cases analyzed by strain from January to June 2006 (A). The second part (B) shows these same urban census tracts but focuses on the incidence rates of dengue cases reported to the Surveillance System from September 2005 to August 2006. https://doi.org/10.1371/journal.pntd.0000448.g009

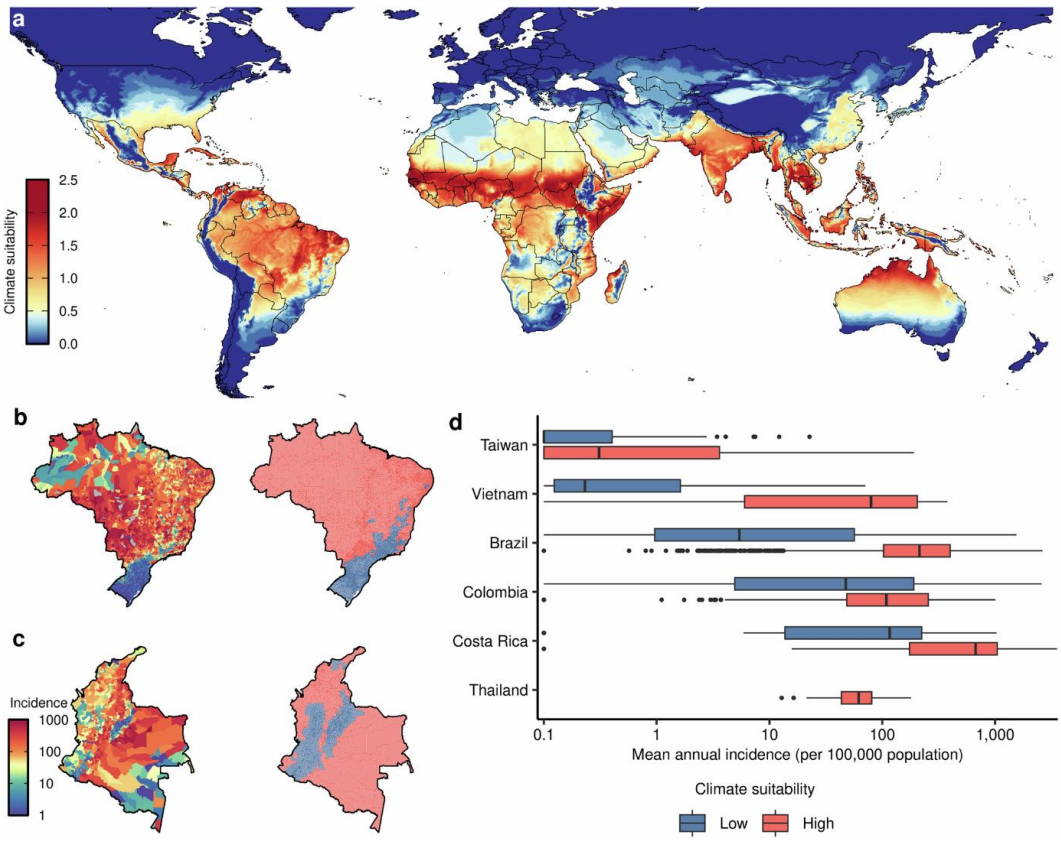

Figure 10. Climate suitability for dengue virus transmission

The average climate conditions that could support dengue virus spread were tracked from 1979 to 2022, based on the Index P scale. We also looked at the yearly averages for dengue cases (measured as cases per 100,000 people; that's in the left panel) and the average climate conditions for dengue transmission (shown in the right panel) across different municipalities in Brazil (with data from 5570 municipalities between 2000 and 2014) and Colombia (1119 municipalities from 2007 to 2017). For clarity, we've marked the climate suitability into two categories: low (<0.5, shown in blue) and high (≥0.5, shown in red). Areas without any incidence data are marked in gray. Lastly, we compared the average number of cases in regions with low versus high climate suitability across various places: Taiwan (districts; 368 areas from 1998 to 2020), Vietnam (provinces; 63 areas from 1997 to 2010), Brazil (municipalities), Colombia (municipalities), Costa Rica (cantons; 82 cantons from 2012 to 2013 and 2015 to 2017), and Thailand (provinces; 77 areas from 2003 to 2022) [32].

Socioeconomic levels of census tracts (quartile)		Low	Inferior Intermediate	Superior Intermediate	High	Total
Molecular analysis (%)*		13 (28.9)	12 (26.7)	9 (20.0)	11 (24.4)	45 (100.0)
Census tracts according quartile of IC (%)**	1°	10 (9.3)	15 (13.9)	29 (26.9)	55 (50.5)	109
	1°-2°	14 (13.0)	27 (25.0)	35 (32.4)	32 (29.4)	108
	2°-3°	3734.3)	28 (25.9)	27 (25.0)	16 (14.7)	108
	3°-4°	47 (43.5)	38 (35.2)	17 (15.7)	6 (5.5)	108
	Total	108 (100.0)	108 (100.0)	108 (100.0)	109 (100.0)	433

*Qui-squared test for non-significant adherence: $\chi^2 = 0.778$; p = 0,8548.
**Qui-squared test for significant independence: $\chi^2 = 101.679$; p<0.0001.
doi:10.1371/journal.pntd.0000448.t001

Table 1. Relationship between the socioeconomic status of census tracts and the incidence rates. https://doi.org/10.1371/journal.pntd.0000448.t001

4. Discussion

The presence of different dengue lineages in SJRP could be due to separate introductions that led to various outcomes or from local genetic diversity developing over time. That's a missed opportunity because this information could really help public health systems manage outbreaks. In our study, we demonstrated how both geographic and time-structured phylogenetic data gives us a clearer picture of how at least two dengue viral lineages are spreading in the urban area of SJRP. That said, we can't pinpoint exactly when the different lineages we discovered came into the picture. SJRP typically sees more rain starting in December, peaking in January and February, right when dengue cases begin to rise, likely alongside Aedes aegypti infestations. It looks like their spread patterns align with the dispersal rates of Aedes aegypti, although there were times when human actions seemed to play a part, too. Certain lineages may disappear from a region due to things like temperature drops, fewer mosquitoes, or shifts in immunity levels during outbreaks. It's pretty fascinating that Aedes aegypti eggs can dry out and still survive, which helps keep the viral strains in play. We also know these strains can come back when the rainy season hits, thanks to transovarial transmission, which is crucial for the virus to stick around in the environment. During the peak of dengue transmission, we saw two main lineages show up, which was right in the middle of the hottest and most humid weather. Then, a third lineage, marked in green in Figures 4, 5, and 6, showed up later in May when the temperatures, rainfall, and humidity all started to drop. We're not really sure if this third lineage could set up for good since we couldn't trace any links to other samples after our data collection ended in July 2006. It's possible that lineage 2 didn't really take hold or may have faded out since it appeared later, around June 6th, during cooler and drier conditions, which aren't ideal for mosquito larvae. Another factor could be that the number of people who could catch the virus was decreasing as the outbreak went on. Looking at the distance matrices in Figure 4, you'll notice that each sample is pretty close to the others, especially considering where and when they were collected and their genetic backgrounds Most cases up until July pointed back to two viral strains sampled in

January and February. On average, our samples were about 3.75 kilometers apart, and the speed of virus spread varied anywhere from zero to around 428.8 meters per day. The Aedes aegypti mosquito tends to drop its eggs in various locations (a behavior known as skip oviposition), which helps maximize its potential for spread and survival. Still, what our findings highlight is that both mosquito movement and human activity are crucial in how the virus disperses, aligning well with earlier estimates that suggested dispersion distances of 15 to 800 meters. And from that, we can glean other useful insights, like the speed and direction of transmission. Each sample tells its own unique story, but by themselves, they don't really show us the full picture of how dengue is acting in São José do Rio Preto. We need to bring together all this data—like timing, location, and genetics—while making some sensible assumptions (for instance, assuming that every sample is connected through lineage or has close genetic relationships with older samples) to start forming a clearer view of how dengue is spreading.

DENV-3 was isolated for the first time in São José do Rio Preto back in January 2006. Our findings suggest that the two lineages diverged roughly one to three years prior to collecting the last sample. Over the four years shown in Figure 2, we observed that after DENV-2 was introduced in 1998, the incidence of dengue started to decline each year. This likely happened because there weren't many susceptible hosts left, but DENV-2 was still present as of June 2005. It seems that DENV-3 might have entered the naive population in SJRP around 2005; in September of that year, a neighborhood in the northern part of the city reported a notable rise in dengue cases. The outbreak extended through October and November and peaked in April 2006. The suggestion that DENV-3 began spreading from the Santa Clara neighborhood in September 2005 and then moved throughout the municipality (as shown in Figure 8) aligns with our results in Figures 2A and 3A. This neighborhood, being underdeveloped, was a likely starting point for transmission, especially since studies on Aedes aegypti larvae infestation from January 2005 [33] showed that lower-income areas with poor sanitation had higher infestation rates compared to wealthier neighborhoods. The widespread dengue transmission across the municipality corresponds to the high R0 values we found, likely because the population was susceptible to serotype 3. One interesting detail is that the BSL (Figure 2A) aligned closely with viral sequences, accurately reflecting the dynamics of the epidemics based on case reports (Figure 2B). However, the peak identified by the BSL occurred around February, which was two months earlier than the highs noted in case reports in April (Figure 2). This could be explained by the use of clinical diagnostics alongside serology up until March 2006, which improves the accuracy of dengue diagnosis. After dengue cases surpassed 300 per 100,000 residents in April 2006, only clinical criteria were used for diagnosis, possibly leading to an uptick in false positives due to the absence of serological verification. These findings reinforce the value of using viral gene genealogies to deduce epidemiological factors for DENV specifically, as well as for rapidly evolving viruses more broadly. Using home addresses to geo-position our patients for the spatial analysis made sense since people spend a lot of time at home, a likely spot for transmission. Still, transmission could happen in other locations too, which might have influenced our data in ways we can't fully account for. However, the exercise was useful, as it revealed consistent transmission patterns that could inform control measures. Our molecular data also indicated that the viral spread wasn't solely reliant on vector movements. The exponential growth phase linked with transmission events beyond typical mosquito flight ranges may have been driven by under-sampling and the movement of infected humans, but it clearly showed rapid transmission among susceptible people. Therefore, it's crucial for surveillance systems to proactively track initial low transmission levels, spot early signs of new serotypes, and map where infected individuals are, ideally before outbreaks escalate. While we didn't find strong connections between dengue cases from molecular analyses and socioeconomic status (Table 1 and Figure 9A), the initial samples that marked the outbreak's start, which likely served as source nodes for many other samples, were mostly in lower-income regions. There's evidence that transmission rates are higher in poorer areas of SJRP, particularly in the north [34]. So, it's worth exploring whether transmission in these regions contributes to a wider spread of the virus within the city. The connection between higher dengue rates and lower socioeconomic levels is mixed. Some studies have shown that poverty correlates with high dengue incidence [35,36], while others haven't [37,38,39] and some even suggest an inverse relationship [40]. One study [48][35] indicated that dengue was more prevalent in poorer neighborhoods of SJRP in 1995, but from 1998 to 2002, after DENV-2's introduction, the best predictor of dengue cases was the proportion of single-story homes. Over the years, socioeconomic factors seemed less relevant, while the spatial characteristics of these areas became more important [41]. Higher dengue transmission in poorer northern areas was noted again during 2005–2006 [34]. Two possible explanations could clarify the mixed patterns of dengue transmission. In both the 1995 and 2006 outbreak seasons, dengue spread initially from poorer northern regions of the city in the preceding years (1994 and 2005) before reaching other areas [5,35] Thus, the highest initial incidence in the north and the lowest in other regions may be tied to delayed control measures at the outbreak's onset. Another possibility is that dengue first took hold in poorer neighborhoods and then spread throughout the city due to a drop in susceptible individuals in the initially affected areas, leading to more equal transmission rates over time. This has been previously documented [42] for the period from 1994 to 1998 when only DENV-1 circulated, though the same wasn't true for the 1998 to 2002 period when both DENV-1 and DENV-2 were present together. The emergence of new DENV serotypes and genotypes poses a significant risk for severe dengue cases [43]. However, it remains debated whether DENV strains leading to severe disease outcompete less virulent ones, which is concerning [18]. Thus, it's crucial to further investigate whether differences in how the virus spreads are related to viral fitness, strain competition, and ultimately, if any of this tie back to increased severity of the disease. We've shown that using Geographic Information Systems for spatial analysis can provide valuable insights into dengue transmission and it's spread within a specific but varied urban landscape, typical of developing nations.

We think this study has really helped us identify infection hotspots more accurately, giving us a clearer picture of how outbreaks unfold and how dengue spreads in SJRP. By bringing together molecular epidemiology and spatial analysis, and by looking into the biological traits and breeding habits of Aedes aegypti mosquitoes, we can better understand the dynamics and transmission of various dengue viral strains [5,32].

5. Conclusion and Future Work

This study takes a close look at how DENV-3 behaved genetically, spatially, and over time during the dengue outbreak in São José do Rio Preto, Brazil, back in 2006. By using molecular phylogenetic techniques and geospatial mapping, we discovered several co-existing DENV-3 lineages, each showing unique patterns of transmission and evolution. What we found here suggests that the rise and prevalence of DENV-3 in the recent epidemics isn't just a fluke; it's actually linked to the virus's ability to adapt and spread effectively in crowded urban areas.

This research combines molecular epidemiology with GIS to uncover transmission patterns that traditional surveillance might miss. Using these approaches is crucial for improving early-warning systems, shaping targeted vector control efforts, and boosting public health strategies, especially in areas that are economically disadvantaged.

This research dives into the genetic, spatial, and timing aspects of DENV-3 during the 2006 dengue outbreak in São José do Rio Preto, Brazil. By using phylogenetic reconstruction, mapping the spread over time and space, and estimating the reproductive number, we showed that several DENV-3 lineages made their way into the area, each with its own unique growth and spread patterns. This research shows that the rise of DENV-3 in recent outbreaks isn’t just a random occurrence; it stems from its ability to evolve and keep spreading in urban areas where people are more susceptible.

Going forward, future studies should really focus on how different DENV serotypes and genotypes interact, especially to figure out if they compete or work together during outbreaks. It’ll also be crucial to dive deeper into how new DENV-3 strains are faring, especially in crowded urban areas.

Mixing molecular epidemiology with geographic information systems proved to be a really effective way to uncover transmission patterns that regular monitoring might overlook. This study highlights just how important it is to have early detection systems, continuous genomic tracking, and targeted vector control efforts, especially in poorer areas where outbreaks could kick off and get worse. Future research should dive into how different strains perform together and their potential dangers, and also think about vaccine strategies that can keep up with changing serotypes and genotypes. By blending various fields, public health systems can gear up to better manage and lessen the impacts of dengue outbreaks associated with DENV-3.

Acknowledgment

The author accepts the support of the Department of Computer Science and Engineering, International Islamic University Chittagong, and appreciates the contribution of global researchers, whose genomic data and epidemiological insights were important for this paper.

References

[1] WHO (1997) Dengue Haemorrhagic Fever. Diagnosis, treatment, prevention and control: WHO - World Health Organization.
[2] Monath TP, Heinz FX (1996) Flaviviruses. In: Fields BN, Knipe DM, Howley PM, editors. Virology. Philadelphia: Lippicott-Raven Publishers. pp. 961–1034.
[3] Zanotto PMA, Gould EA (2002) Molecular epidemiology, evolution and dispersal of the genus Flavivirus. In: Leitner T, editor. The Molecular Epidemiology of Human Viruses. Kluwer Academic Press. pp. 167–195.
[4] Innis B (1995) Dengue and dengue hemorrhagic fever. In: Porterfield JS, editor. Kass Handbook of Infectious Diseases: Exotic Virus Infections. 1st edition. London: Chapman and Hall Medical. pp. 103–146.
[5] Mondini A, Chiaravalloti Neto F, Gallo y Sanches M, Lopes JC (2005) [Spatial analysis of dengue transmission in a medium-sized city in Brazil]. Rev Saude Publica 39: 444–451. https://www.scielosp.org/pdf/rsp/2005.v39n3/444-451/en
[6] Jarman RG, Holmes EC, Rodpradit P, Klungthong C, Gibbons RV, et al. (2008) Microevolution of Dengue viruses circulating among primary school children in Kamphaeng Phet, Thailand. J Virol 82: 5494 – 5500. https://journals.asm.org/doi/abs/10.1128/jvi.02728-07
[7] Chambers TJ, Hahn CS, Galler R, Rice CM (1990) Flavivirus genome organization, expression, and replication. Annu Rev Microbiol 44: 649–688. https://www.cabidigitallibrary.org/doi/full/10.5555/19920512261
[8] Twiddy SS, Holmes EC, Rambaut A (2003) Inferring the rate and time-scale of dengue virus evolution. Mol Biol Evol 20: 122–129.
[9] CVE (2008) [Confirmed autochthonous dengue cases per municipality and per epidemiological week in 2007 in the State of São Paulo]. Centro de Vigilância Epidemiológica.
[10] Holmes EC, Twiddy SS (2003) The origin, emergence and evolutionary genetics of dengue virus. Infect Genet Evol 3: 19–28. https://www.sciencedirect.com/science/article/pii/S1567134803000042
[11] Diaz FJ, Black WCt, Farfan-Ale JA, Lorono-Pino MA, Olson KE, et al. (2006) Dengue virus circulation and evolution in Mexico: a phylogenetic perspective. Arch Med Res 37: 760 – 773. https://www.sciencedirect.com/science/article/pii/S0188440906000890
[12] Messer WB, Gubler DJ, Harris E, Sivananthan K, de Silva AM (2003) Emergence and global spread of a dengue serotype 3, subtype III virus. Emerg Infect Dis 9: 800–809. https://pmc.ncbi.nlm.nih.gov/articles/PMC3023445/

[13] Bennett SN, Holmes EC, Chirivella M, Rodriguez DM, Beltran M, et al. (2003) Selection-driven evolution of emergent dengue virus. Mol Biol Evol 20: 1650–1658. https://academic.oup.com/mbe/article-abstract/20/10/1650/1164131

[14] Zaki A, Perera D, Jahan SS, Cardosa MJ (2008) Phylogeny of dengue viruses circulating in Jeddah, Saudi Arabia: 1994 to 2006. Trop Med Int Health 13: 584–592. https://onlinelibrary.wiley.com/doi/abs/10.1111/j.1365-3156.2008.02037.x

[15] King CC, Chao DY, Chien LJ, Chang GJ, Lin TH, et al. (2008) Comparative analysis of full genomic sequences among different genotypes of dengue virus type 3. Virol J 5: 63. https://link.springer.com/article/10.1186/1743-422X-5-63

[16] Vasilakis N, Holmes EC, Fokam EB, Faye O, Diallo M, et al. (2007) Evolutionary processes among sylvatic dengue type 2 viruses. J Virol 81: 9591–9595. https://journals.asm.org/doi/abs/10.1128/jvi.02776-06

[17] Zhang C, Mammen MP Jr, Chinnawirotpisan P, Klungthong C, Rodpradit P, et al. (2006) Structure and age of genetic diversity of dengue virus type 2 in Thailand. J Gen Virol 87: 873 – 883. https://www.microbiologyresearch.org/content/journal/jgv/10.1099/vir.0.81486-0

[18] Salda LT, Parquet MD, Matias RR, Natividad FF, Kobayashi N, et al. (2005) Molecular epidemiology of dengue 2 viruses in the Philippines: genotype shift and local evolution. Am J Trop Med Hyg 73: 796 – 802. https://nagasaki-u.repo.nii.ac.jp/?action=pages_view_main&active_action=repository_view_main_item_detail&item_id=18295&item_no=1&page_id=13&block_id=21

[19] Pires Neto RJ, Lima DM, de Paula SO, Lima CM, Rocco IM, et al. (2005) Molecular epidemiology of type 1 and 2 dengue viruses in Brazil from 1988 to 2001. Braz J Med Biol Res 38: 843 – 852. https://www.scielo.br/j/bjmbr/a/RwFVfstGrgs54mqR8LRPLHL/?lang=en

[20] Klungthong C, Zhang C, Mammen MP Jr, Ubol S, Holmes EC (2004) The molecular epidemiology of dengue virus serotype 4 in Bangkok, Thailand. Virology 329: 168–179. https://www.sciencedirect.com/science/article/pii/S0042682204005215

[21] Uzcategui NY, Comach G, Camacho D, Salcedo M, Cabello de Quintana M, et al. (2003) Molecular epidemiology of dengue virus type 3 in Venezuela. J Gen Virol 84: 1569 – 1575. https://www.microbiologyresearch.org/content/journal/jgv/10.1099/vir.0.18807-0

[22] de Morais Bronzoni RV, Baleotti FG, Ribeiro Nogueira RM, Nunes M, Moraes Figueiredo LT (2005) Duplex reverse transcription-PCR followed by nested PCR assays for detection and identification of Brazilian alphaviruses and flaviviruses. J Clin Microbiol 43: 696–76 https://journals.asm.org/doi/abs/10.1128/jcm.43.2.696-702.2005

[23] Zwickl D (2006) Genetic algorithm approaches for the phylogenetic analysis of large biological sequence datasets under the maximum likelihood criterion. Austin: The University of Texas.

[24] Swofford DL (2002) PAUP*. Phylogenetic Analysis Using Parsimony (*and Other Methods). Version 4.0 ed. Sunderland, Massachussets: Sinauer Associates.

[25] Drummond AJ, Rambaut A (2006) BEAST 1.4.

[26] Mantel N (1967) The detection of disease clustering and a generalized regression approach. Cancer Res 27: 209 – 220. https://aacrjournals.org/cancerres/article-abstract/27/2_Part_1/209/476508

[27] Anderson RMMR (1991) Infectious Diseases of Humans: Dynamics and Control. New York

[28] Massad E, Coutinho FA, Burattini MN, Lopez LF (2001) The risk of yellow fever in a dengue-infested area. Trans R Soc Trop Med Hyg 95: 370–374. https://www.sciencedirect.com/science/article/pii/S0035920301901841

[29] De Azevedo Neto RS, Silveira AS, Nokes DJ, Yang HM, Passos SD, et al. (1994) Rubella seroepidemiology in a non-immunized population of Sao Paulo State, Brazil. Epidemiol Infect 113: 161 – 173. https://www.cambridge.org/core/journals/epidemiology-and-infection/article/rubella-seroepidemiology-in-a-nonimmunized-population-of-sao-paulo-state-brazil/A85A55EFD1F65ACCFC0CC5CEABB75CBA

[30] Coutinho FA, Massad E, Burattini MN, Yang HM, de Azevedo Neto RS (1993) Effects of vaccination programmes on transmission rates of infections and related threshold conditions for control. IMA J Math Appl Med Biol 10: 187 – 206. https://academic.oup.com/imammb/article-abstract/10/3/187/666912

[31] Massad E, Burattini MN, Coutinho FA, Lopez LF (2003) Dengue and the risk of urban yellow fever reintroduction in Sao Paulo State, Brazil. Rev Saude Publica 37: 477–484. https://www.scielosp.org/pdf/rsp/2003.v37n4/477-484/en

[32] T. Nakase, M. Giovanetti, U. Obolski, and J. Lourenço, "Population at risk of dengue virus transmission has increased due to coupled climate factors and population growth," Commun. Earth Environ., vol. 5, no. 1, Art. 475, Dec. 2024 https://www.google.com/url?sa=t&source=web&rct=j&opi=89978449&url=https://www.nature.com/articles/s43247-024-01639-6&ved=2ahUKEwiMtPKZtdKOAxXQ-TgGHb5JBdYQFnoECBcQAQ&usg=AOvVaw21Kt0o6nWrLgcINilqIrxw

[33] Ferreira AC, Chiaravalloti Neto F (2007) [Infestation of an urban area by Aedes aegypti and relation with socioeconomic levels]. Rev Saude Publica 41: 915–922. https://www.cabidigitallibrary.org/doi/full/10.5555/20083082459

[34] Galli B, Chiaravalloti Neto F (2008) [Temporal-spatial risk model to identify areas at high-risk for occurrence of dengue fever]. Rev Saude Publica 42: 656–663. https://www.scielo.br/j/rsp/a/HXv9JrmhX7FMdt3tWz6CrBP/?lang=en

[35] da Costa AI, Natal D (1998) [Geographical distribution of dengue and socioeconomic factors in an urban locality in southeastern Brazil]. Rev Saude Publica 32: 232 – 236. https://www.scielo.br/j/rsp/a/wvzJGdfCKHSQSzG5WYg8wYR/abstract/?lang=en

[36] Reiter P, Lathrop S, Bunning M, Biggerstaff B, Singer D, et al. (2003) Texas lifestyle limits transmission of dengue virus. Emerg Infect Dis 9: 86–89. https://pmc.ncbi.nlm.nih.gov/articles/PMC2873752/

[37] Bartley LM, Carabin H, Vinh Chau N, Ho V, Luxemburger C, et al. (2002) Assessment of the factors associated with flavivirus seroprevalence in a population in Southern Vietnam. Epidemiol Infect 128: 213 – 220. https://www.cambridge.org/core/journals/epidemiology-and-infection/article/assessment-of-the-factors-associated-with-flavivirus-seroprevalence-in-a-population-in-southern-vietnam/F77597208E2004E32F9AB6CB44F97F89

[38] Espinoza-Gomez F, Hernandez-Suarez CM, Rendon-Ramirez R, Carrillo-Alvarez ML, Flores-Gonzalez JC (2003) [Interepidemic transmission of dengue in the city of Colima, Mexico]. Salud Publica Mex 45: 365 – 370. https://www.scielo.org.mx/scielo.php?pid=S0036-36342003000500006&script=sci_abstract&tlng=en

[39] Teixeira Mda G, Barreto ML, Costa Mda C, Ferreira LD, Vasconcelos PF, et al. (2002) Dynamics of dengue virus circulation: a silent epidemic in a complex urban area. Trop Med Int Health 7: 757 – 762. https://onlinelibrary.wiley.com/doi/abs/10.1046/j.1365-3156.2002.00930.x

[40] Vasconcelos PF, Lima JW, da Rosa AP, Timbo MJ, da Rosa ES, et al. (1998) [Dengue epidemic in Fortaleza, Ceara: randomized seroepidemiologic survey]. Rev Saude Publica 32: 447–454. https://europepmc.org/article/med/10030061

[41] Mondini A, Chiaravalloti-Neto F (2008) Spatial correlation of incidence of dengue with socioeconomic, demographic and environmental variables in a Brazilian city. Sci Total Environ 393: 241 – 248. https://www.sciencedirect.com/science/article/pii/S0048969708000144

[42] Mondini A, Chiaravalloti Neto F (2007) [Socioeconomic variables and dengue transmission]. Rev Saude Publica 41: 923–930. https://www.scielosp.org/pdf/rsp/2007.v41n6/923-930/en

[43] Gubler DJ (1998) Dengue and dengue hemorrhagic fever. Clin Microbiol Rev 11: 480 – 496. https://journals.asm.org/doi/abs/10.1128/cmr.11.3.480